Clipping-Enhanced Optical OFDM for IM/DD Communication Systems

Jie Lian and Maïté Brandt-Pearce
Charles L. Brown Department of Electrical and Computer Engineering
University of Virginia, Charlottesville, VA 22904
Email: jl5qn@virginia.edu, mb-p@virginia.edu

division multiplexing Abstract—Orthogonal frequency (OFDM) is a candidate technique to provide high-speed data transmissions for optical communication systems. For intensity modulation and direct detection (IM/DD) optical communication systems, the peak transmitted power limitation of light sources and nonnegative transmitted signal constraints can result in nonlinear distortions from clipping. In this paper, we propose a clipping enhanced optical OFDM (CEO-OFDM) for IM/DD communication systems to reduce the clipping effects. CEO-OFDM transmits the information that results from clipping the peak power, which allows the use of a higher modulation index to improve the signal to noise ratio in exchange for a larger bandwidth. For the same transmitted data rate, CEO-OFDM can achieve a lower bit error rate than DC-biased optical OFDM (DCO-OFDM), asymmetrically clipped optical OFDM (ACO-OFDM) and unipolar OFDM (U-OFDM). By using a larger modulation constellation size, the proposed CEO-OFDM can support a higher throughput than other techniques when the same bit error rate is achieved.

Index Terms—IM/DD optical communication, clipping distortion, power constraint, OFDM

I. INTRODUCTION

Intensity modulation and direction detection (IM/DD) systems have attracted much attention in recent optical wireless communications research due to their many advantages over radio-frequency (RF) communications [1], [2]. Compared to conventional RF communications, optical wireless communications are immune to RF interference, can offer higher security, can provide potentially high-data-rate transmission, and the spectrum is not regulated. IM/DD has also often been used for fiber-optic systems when coherent systems incur too high a cost or complexity.

The natural properties of laser diodes (LDs) and photodetectors (PDs) require the transmitted and received signals to be real-valued. If IM/DD is used for LD-based communication systems, the transmitted signals must be non-negative. These properties constrain the modulation that can be employed. Recently, orthogonal frequency division multiplexing (OFDM) has been proposed for IM/DD systems due to its resistance to inter-symbol interference (ISI) and high spectral efficiency [3], [4]. In this paper, we propose a new optical OFDM technique for IM/DD systems that can provide a better bit error rate (BER) performance than other currently proposed methods.

Since the transmitted signal must be real and non-negative, conventional OFDM cannot be applied directly in LD-based communication systems. There are some popular optical OFDM techniques that are designed for IM/DD systems. DC biased optical OFDM (DCO-OFDM) is the most commonly used optical OFDM techniques [5]. To make the bipolar OFDM signal unipolar, a DC-bias (usually half of the peak transmitted power) must be added. However, the DC bias requires extra power, and negative signals cannot be totally avoided. Asymmetrically clipped optical OFDM (ACO-OFDM) is designed for optical communications, and requires less power than DCO-OFDM [6], [7]. In ACO-OFDM, only odd subcarriers are used to modulate the signals, and the even subcarriers are blank. A DC bias is not required for ACO-OFDM. Combining the ACO-OFDM with pulse position modulation, some researchers proposed fractional reverse polarity optical OFDM, which takes dimming control into consideration [8]. Unipolar OFDM (U-OFDM) is a recently proposed alternative technique that can generate unipolar signals without adding a DC signal [9]. In U-OFDM systems, the light sources first transmit the positive part of the bipolar original OFDM signal. After that, the negative part of the signal is transmitted.

For IM/DD systems, a required limit on the light sources' peak transmitted power can introduce severe peak clipping distortion for high valued signals. DCO-OFDM has both zero and peak clipping distortion. The peak power constraint can impact ACO and U-OFDM and introduce unrecoverable distortions. In this paper, a clipping enhanced optical OFDM (CEO-OFDM) is proposed to transmit the clipped information and reduce the distortion caused by the limited peak transmitted power. We optimize the modulation index that controls the scale of the transmitted signals to enhance the signal to noise ratio (SNR) and minimize the BER. By using CEO-OFDM, since the clipping is reduced, a higher modulation index can be applied compared with DCO, ACO and U-OFDM to achieve a better BER performance. From numerical results, for the same BER performance, CEO-OFDM can support higher bit rates than DCO-, ACO- and U-OFDM techniques by using a larger modulation constellation size. In this paper, we assume an ideal transmitter; the bandlimited channel source is beyond the scope of this paper.

The remainder of the paper is organized as follows. Section II describes the nonlinearity of light sources. The principles of CEO-OFDM are described in Section III. The numerical and

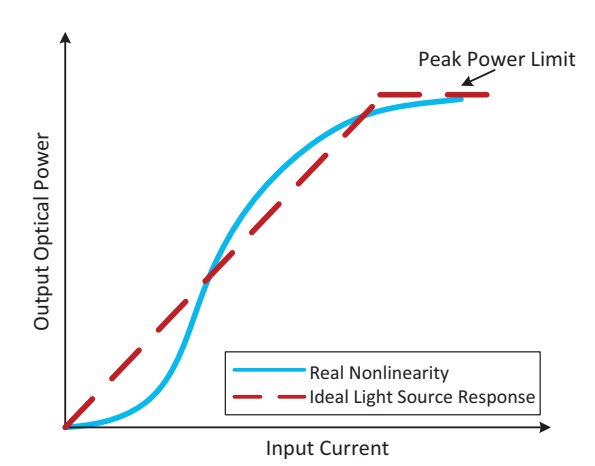


Fig. 1. Ideal clipping and real nonlinearity of light sources.

simulation results are discussed in Section IV. The bandwidth required by the various techniques is addressed in Section V. The paper is concluded in Section VI.

II. NONLINEARITY OF LIGHT SOURCE

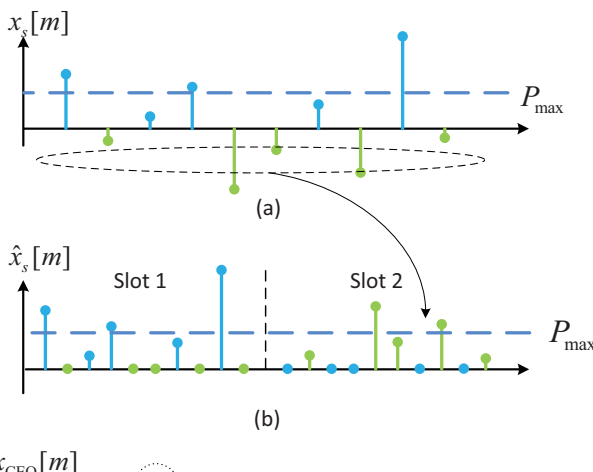
Laser diodes and other light sources that work as transmitters in IM/DD systems are driven by forward current signals. Due to the laser diode's structure, the output optical power and the driving input current are nonlinearly related. The maximum output optical signal from the LD is limited by a peak power constraint, which is caused by current saturation, and this can result in the clipping of large peaks in the modulated signal. As shown in Fig. 1, the nonlinearity of the LDs can introduce a distortion if multilevel or continuous valued signals are transmitted in IM/DD systems [10].

To linearize the relation between the output optical power and the input current, predistortion is a possible solution [10], [11]. As shown in Fig. 1, after predistortion, the real nonlinearity can be linearized as a linear function within a range of input values, behaving as an ideal light source. The zero and peak power constraints must clip the signals beyond this linear range. In this paper, we assume that predistortion is employed.

III. CEO-OFDM DESCRIPTION

This section describes the principle of CEO-OFDM and analyzes its performance. CEO-OFDM can reduce clipping distortion by transmitting the positive, negative and clipped information successively.

Fig. 2 illustrates the basic principle of CEO-OFDM. After using Hermitian symmetry, the bipolar real OFDM signal is shown in Fig. 2 (a). Positive and negative signals of the bipolar signal are transmitted successively in time slots 1 and 2, as in U-OFDM, shown in Fig. 2 (b). In CEO-OFDM, shown in Fig. 2 (c), the high-valued signals in slots 1 and 2 that are clipped by the peak power constraint ($P_{\rm max}$) are transmitted in time slot 3. To guarantee the CEO-OFDM signal can be recovered perfectly at the receiver, time slots 1, 2 and 3 have the same



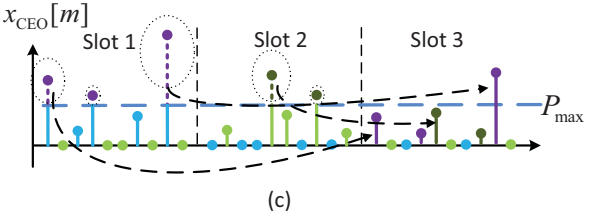


Fig. 2. Illustration of OFDM signals. (a) bipolar OFDM signal, (b) unipolar OFDM signal (U-OFDM), (c) CEO-OFDM signal.

length. Therefore, the modulation bandwidth of CEO-OFDM is $3R_b/\log_2 M$, where R_b and M are the transmitted bit rate and modulation constellation size, respectively.

The block diagram of the proposed CEO-OFDM is shown in Fig. 3. To simplify the notation, we analyze the signal in one symbol time. For CEO-OFDM, M-ary quadrature amplitude modulation (M-QAM) is applied, where M is the modulation constellation size. We assume that X_i is the data at the after M-QAM for the ith subcarrier. To make the transmitted signals real, X_i must be the conjugate of X_{N-i} , $X_{N-i} = X_i^*$, $\forall i = 0, \cdots, N-1$, where N is the number of subcarriers. The vector $\mathbf{X} = (X_0, X_1, \cdots, X_{N-1})^T$ is the input to an inverse fast Fourier transform (IFFT), where the output is denoted as x[k] that can be represented as

$$x[k] = \frac{c}{N} \sum_{i=0}^{N-1} X_i \exp\left(\frac{j2\pi ki}{N}\right),\tag{1}$$

where c is a variable used to set the modulation index, c/N. After the parallel to serial converter, the mth sample of the symbol can be represented as $x_s[m] = \sum_{k=0}^{N-1} x[k] \delta[m-k]$. An example of the bipolar signal $x_s[m]$ is shown in Fig. 2 (a). After flipping the negative part of $x_s[m]$ and placing it after the positive signal, the bipolar signal can be converted to a unipolar signal, $\hat{x}_s[m]$, which can be represented as

$$\hat{x}_s[m] = \underbrace{g(x_s[m])}_{x_s^{(+)}[m]} + \underbrace{g(-x_s[m-N])}_{x_s^{(-)}[m]},\tag{2}$$

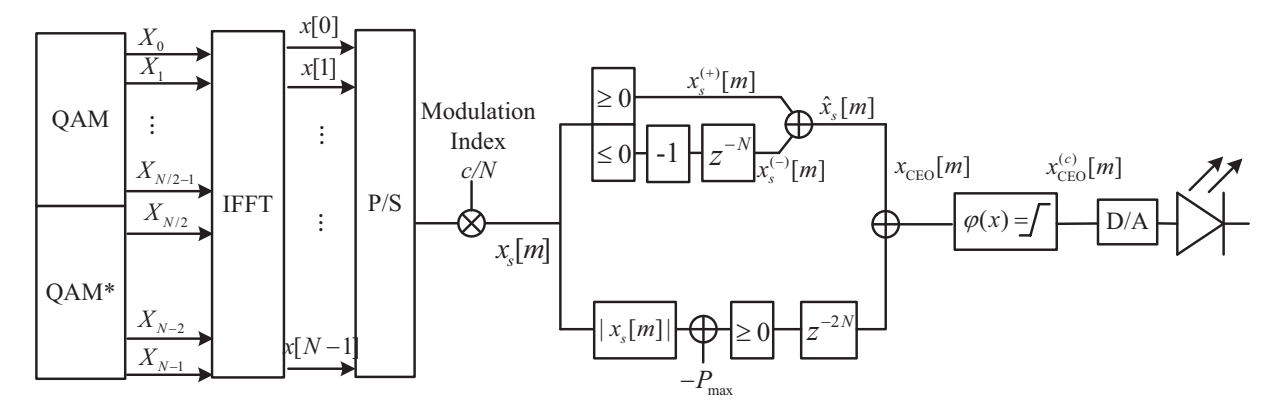


Fig. 3. Block diagram of the transmitter in CEO-OFDM systems.

where the function g(x) is defined as

$$g(x) = \begin{cases} x, & x > 0 \\ 0, & x \le 0 \end{cases} . \tag{3}$$

As shown in Fig. 2 (b), $\hat{x}_s[m]$ includes both the positive and negative information of $x_s[m]$. The parts greater than P_{\max} are clipped and transmitted in slot 3, which is shown in Fig. 2 (c). Therefore, any remaining hard clipping can only happen in slot 3. Then, the CEO-OFDM signal for each symbol can be represented as

$$x_{\text{CEO}}[m] = \underbrace{g(x_s[m])}_{\text{slot 1}} + \underbrace{g(-x_s[m-N])}_{\text{slot 2}}, m = 0, \dots, 3N - 1$$
$$+ \underbrace{g(|x_s[m-2N]| - P_{\text{max}})}_{\text{slot 3}}, m = 0, \dots, 3N - 1$$

After clipping, the transmitted signal is

$$x_{\text{CEO}}^{(c)}[m] = \varphi\left(x_{\text{CEO}}[m]\right),$$
 (5)

where

$$\varphi(x) = \begin{cases} P_{\text{max}}, & x > P_{\text{max}} \\ x, & 0 < x \le P_{\text{max}} \end{cases} . \tag{6}$$

When N is large (usually greater than 64), the real OFDM signal $x_s[m]$ can be modeled as a Gaussian distributed random variable with zero mean and variance σ_x^2 [12]. Thus, the clipped CEO-OFDM signal, $x_{\rm CEO}^{(c)}[m]$, can be modeled as a random variable with a probability density function (pdf)

$$\begin{split} f_{\mathrm{C}}(x) &= \frac{2}{3\sqrt{2\pi}\sigma_x} \left(\exp\left(\frac{-x^2}{2\sigma_x^2}\right) + \exp\left(\frac{-(x+P_{\mathrm{max}})^2}{2\sigma_x^2}\right) \right) \\ &+ \frac{1}{3} \left(\operatorname{erfc}\left(\frac{P_{\mathrm{max}}}{\sqrt{2}\sigma_x}\right) + \operatorname{erfc}\left(\frac{\sqrt{2}P_{\mathrm{max}}}{\sigma_x}\right) \right) \delta(x-P_{\mathrm{max}}) \\ &+ \frac{1}{3} \left(2 - \operatorname{erfc}\left(\frac{P_{\mathrm{max}}}{\sqrt{2}\sigma_x}\right) \right) \delta(x), \end{split}$$

where $\operatorname{erfc}(\cdot)$ is the complementary error function, which is defined as $\operatorname{erfc}(x) = 2/\sqrt{\pi} \int_x^\infty \exp(-u^2) \mathrm{d}u$. An example

of the simulated and theoretical probability density function for CEO-OFDM is shown in Fig. 4, where we note that the simulated and the theoretical results agree. Due to the peak power constraint, the signal is distributed in the range $[0,P_{\rm max}].$

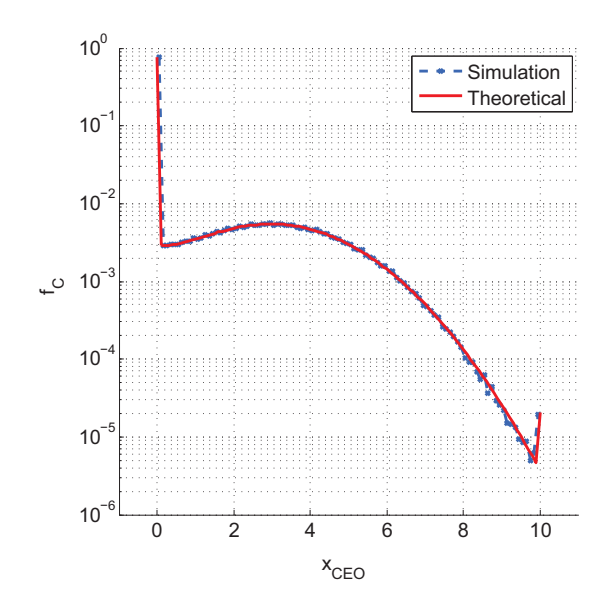


Fig. 4. Simulated and theoretical pdf of clipped CEO-OFDM signals. $P_{\rm max}$ =10 mW, c/N=0.3125,~N=64.

Due to the peak power limit of the light source, some of the CEO-OFDM signal with large amplitude may be clipped. The clipped signal can be modeled by using the Bussgang theorem, which can be represented as [13],

$$x_{\text{CEO}}^{(c)}[m] = \alpha \cdot x_{\text{CEO}}[m] + n_{\text{clip}}[m],$$

$$m = 2N, \dots, 3N - 1$$
(8)

where α is a constant coefficient that can be calculated from

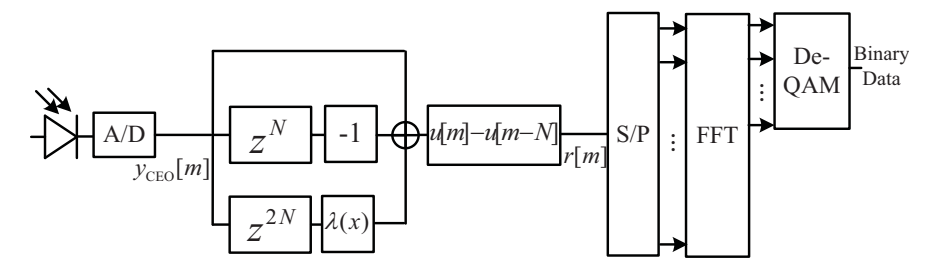


Fig. 5. CEO-OFDM receiver structure

[13] as

$$\alpha = \frac{1}{\sigma_x^3 \sqrt{2\pi}} \int_{-\infty}^{\infty} x \psi(x) \exp\left(-\frac{x^2}{2\sigma_x^2}\right) dx$$

$$= 1 - \operatorname{erfc}\left(\frac{2P_{\text{max}}}{\sqrt{2}\sigma_x}\right),$$
(9)

where $\psi(x)$ is a nonlinear function that can be represented as

$$\psi(x) = \begin{cases} -2P_{\text{max}}, & x < -2P_{\text{max}} \\ x, & -2P_{\text{max}} < x < 2P_{\text{max}} \\ 2P_{\text{max}}, & x > 2P_{\text{max}}. \end{cases}$$
(10)

The additive term $n_{\rm clip}[m]$ can be modeled as noise caused by the clipping effects with variance

$$\sigma_{\text{clip}}^{2} = \int_{P_{\text{max}}}^{\infty} (x - P_{\text{max}})^{2} f_{\text{C}}(x) dx.$$

$$= \frac{1}{6} \left(4P_{\text{max}}^{2} + \sigma_{x}^{2} \right) \left(1 - \text{erfc} \left(\frac{\sqrt{2}P_{\text{max}}}{\sigma_{x}} \right) \right)$$

$$+ \frac{1}{6} \left(P_{\text{max}}^{2} + \sigma_{x}^{2} \right) \left(1 - \text{erfc} \left(\frac{P_{\text{max}}}{\sqrt{2}\sigma_{x}} \right) \right)$$

$$+ \frac{1}{6} P_{\text{max}}^{2} - \frac{1}{6} \sqrt{\frac{2}{\pi}} \sigma_{x} P_{\text{max}} \exp \left(\frac{-P_{\text{max}}}{2\sigma_{x}^{2}} \right)$$

$$+ \frac{1}{3} \sqrt{\frac{2}{\pi}} \sigma_{x} P_{\text{max}} + \frac{1}{3}.$$
(11)

The structure of the CEO-OFDM receiver is illustrated in Fig. 5. In this figure, the discrete version of the received signal can be modeled as

$$y_{\text{CEO}}[m] = \rho h(\alpha x_{\text{CEO}}[m] + n_{\text{clip}}[m]) + n[m], \qquad (12)$$

where ρ is the responsivity of the PD at the receiver, and h is the channel loss. n[m] is the additive noise. In this paper, we assume n[m] is the result of Gaussian white noise with zero mean, and variance calculated as $\sigma_{\rm n}^2=3N_0R_s$, where R_s is the transmitted symbol rate, and N_0 is the noise power spectral density. After the received signal is reconstructed, we can model the mth sample of the reconstructed signal in one symbol as

$$\begin{split} r[m] &= (y_{\text{CEO}}[m] - y_{\text{CEO}}[m+N]) \, (u[m] - u[m-N]) \\ &+ \lambda (x_{\text{CEO}}[m]) \cdot y_{\text{CEO}}[m+2N] \cdot (u[m] - u[m-N]), \\ m &= 0, 1, \cdots, N-1 \end{split}$$

(13)

 $\label{eq:TABLE I} \textbf{TABLE I} \\ \textbf{PARAMETERS USED FOR NUMERICAL RESULTS} \\$

Channel loss, h	1
Responsivity, ρ	0.9 A/W
Peak optical power limit, P_{max}	8 mW
Number of subcarriers, N	64
Noise spectral density, N_0	3×10^{-11} mW/Hz
R_b for 32-QAM	1.25 Gbps
R_b for 64-QAM	1.5 Gbps

where u[m] is the discrete format of the unit step function. $\lambda(x)$ is a function used for reconstructing the signal, which can be calculated as

$$\lambda(x) = \begin{cases} 1, & x \neq 0 \\ -1, & x = 0 \end{cases} . \tag{14}$$

In this paper, we assume there is no inter-symbol interference, and the channel loss is assumed to be unity. At the receiver, the subcarrier signal to noise ratio (SNR) can be calculated as

$$\gamma = \frac{(c\alpha h\rho)^2}{N(h^2\rho^2\sigma_{\rm clip}^2 + \sigma_{\rm n}^2)},$$
 (15)

Given the SNR, we can calculate the BER by using the approximate expression [14]

BER
$$\approx \frac{\sqrt{M} - 1}{\sqrt{M} \log_2(\sqrt{M})} \operatorname{erfc}\left(\sqrt{\frac{3\gamma}{2(M-1)}}\right).$$
 (16)

IV. NUMERICAL RESULTS

Numerical results of the performance of the proposed CEO-OFDM are shown in this section. CEO-OFDM is compared with ACO-, DCO- and U-OFDM as benchmarks. To make the comparison fair, the transmitted data rate for techniques that use the same modulation is the same. The results shown are derived from the analysis shown above; they have been validated through simulation. Unless otherwise noted, the parameters used to obtain the numerical results are shown in Table I.

Fig. 6 shows the maximum value of the OFDM signals prior to clipping for different modulation indexes. The maximum magnitude of DCO-, U-, ACO- and CEO-OFDM increases with increasing modulation index. From the results, DCO-OFDM signal has the largest maximum magnitude due

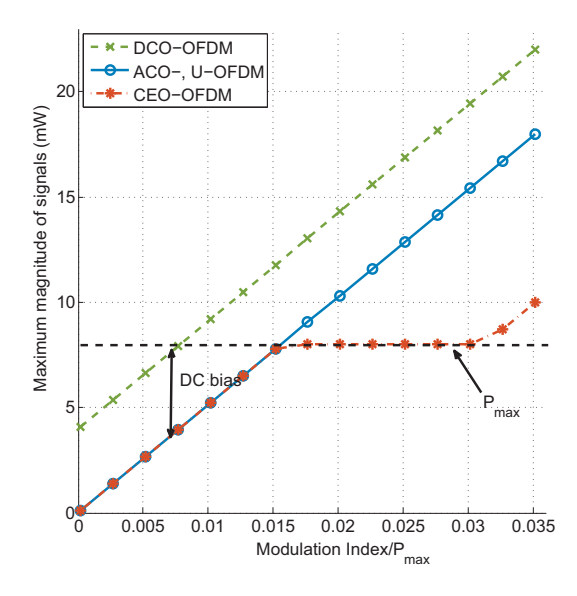


Fig. 6. Maximum magnitude of OFDM signals before clipping.

to the DC bias. ACO- and U-OFDM have the same maximum magnitude value. For CEO-OFDM, the maximum magnitude is same as ACO- and U-OFDM when it is less than the peak power. When the modulation index continues to increase, the maximum magnitude of CEO-OFDM is much less than ACO- and U-OFDM. Therefore, the CEO-OFDM can dramatically reduce the clipping distortion caused by the peak power constraint.

Fig. 7 shows a BER performance comparison of DCO-, ACO-, U- and CEO-OFDM with increasing modulation index. For low modulation index values, the BER performance for all techniques improves as the modulation index increases. Then, after the clipping noise begins to dominate, further increasing the modulation index eventually causes the BER performance to worsen. The BER performance of DCO-OFDM reaches an optimal value when the modulation index is less than 10% of $P_{\rm max}$. Since the transmitted data rate is the same, CEO-OFDM needs 1.5 times more bandwidth than U- and ACO-OFDM, and 3 times more bandwidth than DCO-OFDM, and therefore experiences stronger noise power. The performance of CEO-OFDM is thus worse than the others when the modulation index is relatively small. As the modulation index increases, the potential advantage of CEO-OFDM becomes apparent. Since the clipped information is transmitted, a higher modulation index can be used to provide a higher effective SNR. For DCO-, U- and ACO-OFDM, since a higher modulation index can result in severe clipping noise, the performance is not as good as CEO-OFDM.

By choosing the optimal modulation index, CEO-OFDM can always achieve a better BER performance than DCO-, U- and ACO-OFDM. Fig. 8 shows the minimum BER as the peak power increases using the optimal modulation index for each technique. To achieve the same $\rm BER=10^{-3}$,

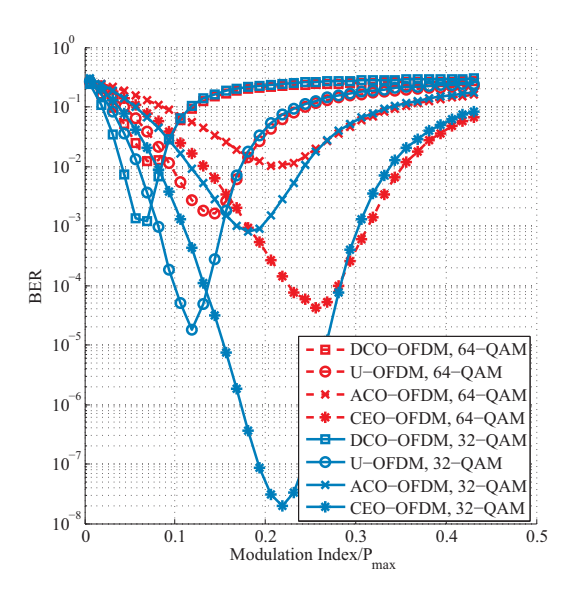


Fig. 7. BER comparison of DCO-, U-, ACO- and CEO-OFDM for different modulation indexes.

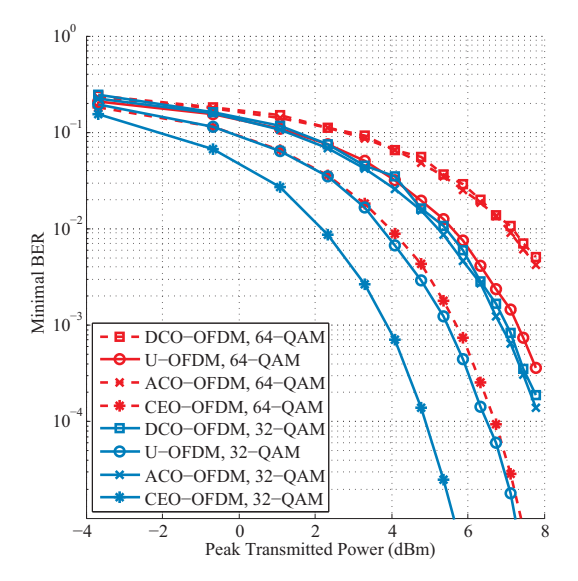


Fig. 8. BER comparison of DCO-, U-, ACO- and CEO-OFDM for different transmitted power.

CEO-OFDM needs 2 dB less power than U-OFDM, and 4 dB less power than ACO- and DCO-OFDM. For a similar BER performance, the transmitted data rate for CEO-OFDM can be 20% higher than for U-OFDM, by using a larger modulation constellation size. Compared with DCO- and ACO-OFDM, the proposed CEO-OFDM can provide a better BER or a higher data transmission rate.

V. BANDWIDTH DISCUSSIONS

In this section, we briefly analyze and compare the bandwidth of the proposed CEO-OFDM and other optical OFDM techniques we mentioned in this paper. We first consider the case that all techniques use the same symbol rate, bit rate and modulation constellation size. Obviously, we can obtain the following relations:

$$\Delta f_{\rm DCO} = \frac{1}{2} \Delta f_{\rm ACO} = \frac{1}{2} \Delta f_{\rm U} = \frac{1}{3} \Delta f_{\rm CEO}, \qquad (17)$$

where $\Delta f_{\rm DCO}$, $\Delta f_{\rm ACO}$, $\Delta f_{\rm U}$ and $\Delta f_{\rm CEO}$ are the required bandwidth for DCO-, ACO-, U- and CEO-OFDM, respectively. From this relationship, the proposed CEO-OFDM requires 3 times and twice the bandwidth than DCO-OFDM and U-OFDM, respectively.

From the numerical results in Fig. 7 we can conclude that CEO-OFDM can achieve a higher SNR by using a higher modulation index, and the higher SNR can support a larger modulation constellation size. Therefore, the larger constellation size can compensate for some of its bandwidth inefficiency. In this paper, we define the bandwidth efficiency as the bit rate per bandwidth (b/s/Hz).

From Fig. 8, we compare the results of 64-QAM for U-OFDM and 32-QAM for DCO and ACO-OFDM. They have a similar BER performance. Therefore, for this case, we can see that

$$\eta_{\rm DCO} = 2 \, \eta_{\rm ACO}$$

$$\eta_{\rm DCO} = 2 \cdot \frac{\log_2 32}{\log_2 64} \, \eta_{\rm U} \approx 1.67 \, \eta_{\rm U}$$
(18)

where the subscripts represent the OFDM prefixes. Comparing the results of 64-QAM for CEO-OFDM and 32-QAM for U-OFDM in Fig. 8, which also have similar performance, we can also obtain that

$$\eta_{\rm U} = \frac{3}{2} \cdot \frac{\log_2 32}{\log_2 64} \, \eta_{\rm CEO} = 1.25 \, \eta_{\rm CEO}.$$
(19)

Therefore, $\eta_{\rm DCO} \approx 2.08 \, \eta_{\rm CEO}$.

In general, for the same bit rate and symbol rate, the proposed CEO-OFDM requires 3 times and twice bandwidth than DCO and U-OFDM, respectively. However, when we take the BER performance into account, the bandwidth efficiency of CEO-OFDM is similar to ACO-OFDM.

VI. CONCLUSION

In this paper, we propose a new OFDM scheme for IM/DD systems we call the clipping enhanced optical OFDM. The proposed CEO-OFDM transmits the information that is clipped by the peak power constraint. By sacrificing bandwidth, CEO-OFDM allows the use of a higher modulation index to improve the SNR. Compared with DCO-, U-,

and ACO-OFDM, CEO-OFDM can achieve a better BER performance when the transmission data rate is the same. In addition, using CEO-OFDM, a larger modulation constellation size can be applied to achieve a higher data rate than other OFDM techniques when the BER performances are the same.

In future work, a dispersive channel and bandlimited light source will be considered. For visible light communication systems, dimming control and the effects of different illumination requirements on CEO-OFDM will be explored.

ACKNOWLEDGEMENT

This work was funded in part by the National Science Foundation (NSF) through the STTR program, under award number 1521387, and VLNComm, Inc.

REFERENCES

- T. Komine and M. Nakagawa, "Fundamental analysis for visible-light communication system using LED lights," *IEEE Trans. on Consumer Electron.*, vol. 50, no. 1, pp. 100–107, Feb 2004.
- [2] A. Jovicic, J. Li, and T. Richardson, "Visible light communication: opportunities, challenges and the path to market," *IEEE Commun. Mag.*, vol. 51, no. 12, pp. 26–32, December 2013.
 [3] A. Azhar, T. Tran, and D. O'Brien, "A Gigabit/s indoor wireless
- [3] A. Azhar, T. Tran, and D. O'Brien, "A Gigabit/s indoor wireless transmission using MIMO-OFDM visible-light communications," *IEEE*, *Photon. Technol. Lett.*, vol. 25, no. 2, pp. 171–174, 2013.
- [4] H. Elgala, R. Mesleh, and H. Haas, "Indoor optical wireless communication: potential and state-of-the-art," *IEEE Commun. Mag.*, vol. 49, no. 9, pp. 56–62, 2011.
- [5] M. Zhang and Z. Zhang, "An optimum DC-biasing for DCO-OFDM system," *IEEE Commun. Lett.*, vol. 18, no. 8, pp. 1351–1354, Aug 2014.
- [6] J. Armstrong and A. J. Lowery, "Power efficient optical OFDM," Elect. Lett., vol. 42, no. 6, pp. 370–372, March 2006.
- [7] J. Armstrong and B. J. C. Schmidt, "Comparison of asymmetrically clipped optical OFDM and DC-biased optical OFDM in AWGN," *IEEE Communications Letters*, vol. 12, no. 5, pp. 343–345, May 2008.
- [8] T. Q. Wang and X. Huang, "Fractional reverse polarity optical OFDM for high speed dimmable visible light communications," *IEEE Trans. on Commun.*, in press, 2018.
- [9] D. Tsonev, S. Sinanovic, and H. Haas, "Novel unipolar orthogonal frequency division multiplexing (U-OFDM) for optical wireless," in 2012 IEEE 75th Vehicular Technology Conference (VTC Spring), May 2012, pp. 1–5.
- [10] M. Noshad and M. Brandt-Pearce, "Hadamard-coded modulation for visible light communications," *IEEE Trans. on Commun.*, vol. 64, no. 3, pp. 1167–1175, March 2016.
- [11] W. Zhao, Q. Guo, J. Tong, J. Xi, Y. Yu, P. Niu, and X. Sun, "Orthogonal polynomial-based nonlinearity modeling and mitigation for LED communications," *IEEE Photonics Journal*, vol. 8, no. 4, pp. 1–12, Aug 2016.
- [12] J. Armstrong, "OFDM for optical communications," Journal of Lightwave Technology, vol. 27, no. 3, pp. 189–204, Feb 2009.
- [13] R. Price, "A useful theorem for nonlinear devices having Gaussian inputs," *IRE Transactions on Information Theory*, vol. 4, no. 2, pp. 69–72, June 1958.
- [14] Z. Ghassemlooy, W. Popoola, and Rajbhandari, Optical Wireless Communications: System and Channel Modeling with Matlab. CRC Press 2013